The effect of detachment and attachment to a kink motion in the asymmetric simple exclusion process

Tetsuya Mitsudo† and Hisao Hayakawa‡

Department of Physics, Yoshida-South campus, Kyoto University, Sakyo-ku, Kyoto, Japan, 606-8501

Abstract. We study the dynamics of a kink in a one-lane asymmetric simple exclusion process with detachment and attachment of the particle at arbitrary sites. For a system with one site of detachment and attachment we find that the kink is trapped by the site, and the probability distribution of the kink position is described by the overdumped Fokker-Planck equation with a V-shaped potential. Our results can be applied to the motion of a kink in arbitrary number of sites where detachment and attachment take place. When detachment and attachment take place at every site, we confirm that the kink motion obeys the diffusion in a harmonic potential. We compare our results with the Monte Carlo simulation, and check the quantitative validity of our theoretical prediction of the diffusion constant and the potential form.

1. Introduction

An asymmetric simple exclusion process (ASEP) is a simple nonequilibrium stochastic lattice model of transport process. ASEP is defined on a one-dimensional lattice, and particles hop to the neighbouring site when the site is empty. The transportation of particles is induced by the asymmetric hopping of the particles. Recently much attention is paid to ASEP [1, 2, 3], not only because there exists the exact solution under the open boundary condition [4, 5, 6, 7], but also it is applicable to various transportation phenomena. In particular, the uni-directional ASEP which is called totally asymmetric simple exclusion process (TASEP) has been studied extensively, because (i) TASEP is the simplest ASEP and (ii) TASEP keeps the essence of nonequilibrium transport processes such as the exclusion interaction between particles and the drift of particles. In fact, TASEP may be regarded as a simplified model of traffic flow [8].

We can also apply ASEP to biological problems. TASEP is first introduced as a model to explain the process of creation of the messenger RNA [9]. The model with detachment and attachment on each site in TASEP with open boundary conditions is known as PFF model [10], named after the authors' names: Parmeggiani, Franosch and Frey. An extended model of the PFF model is used to describe an intra-cellular transport of the single-headed kinesin (KIF1A) motor [11].

† mitsudo@yukawa.kyoto-u.ac.jp
‡ hisao@yukawa.kyoto-u.ac.jp

In the open boundary ASEP, we can draw the phase diagram by the incoming rate and outgoing rate at the boundaries. On the boundary between the low density phase and high density phase, it is known that the kink between a sparse region and a jammed region obeys Brownian motion. This kink motion in one-lane ASEP is also studied in terms of the domain wall theory [12, 13, 14] and the second class particle [15, 16, 17]. The kink motion in a two-lane TASEP is studied in ref.[18], and the kink motion in the PFF model is studied in ref.[19, 20, 21, 22]. It is notable that the kink is trapped by a harmonic potential in the PFF model [19, 20].

In this paper, we discuss the kink motion of TASEP with detachment and attachment. Our method can be used for any number of sites of detachment and the attachment. The effect of detachment of particles at the middle site of the system was studied in ref.[23] by dividing the system into two systems of TASEP, though the kink motion was not discussed there. We demonstrate that one site of detachment and attachment attracts the kink where attractive potential is a linear function of distance from the site of detachment and attachment. Even when we generalize the model with many sites of detachment and attachment, the kink feels the linear combination of the linear potentials for one-site of detachment and attachment. Though the analysis of linear combination of linear potential we derive the harmonic potential in PFF model.

The organization of this paper is as follows. We first introduce the model with detachment and attachment at one site and briefly review previous studies on the kink motion in TASEP without detachment and attachment in section 2. We present a theory of a kink motion in TASEP with detachment and attachment at one site, and extend our analysis to the kink motion in TASEP with detachment and attachment at many sites including the PFF model. In section 3, we compare our analysis with the Monte-Carlo simulation and confirm the quantitative agreement between the theory and the simulation. Finally, we give concluding remarks.

2. The kink motion

2.1. A model for one site of detachment and attachment

Let us explain TASEP model with detachment and attachment of particles at one site under the open boundary conditions. TASEP is defined on a one-dimensional lattice of L sites. Each particle hops forward when the site in front is empty. Here we choose right as the drift direction of particles. The open boundary condition is specified by a particle attachment rate α at the left end of the system and a particle detachment rate β at the right end. Here, the particle is also detached by the rate w_d and attached by the rate w_a at the site x_0. TASEP with detachment at one site has first been introduced in the ref.[23]. They divide the system into two systems of TASEP by the site of the detachment, and introduce the effective hopping rate to connect the two systems at the site x_0 which is fixed to the middle of the system to include the effect of detachment. However, we can not explain the kink localization near x_0 by introducing the effective

hopping rate between two systems because the kink moves under the reflective boundary condition of a virtual boundary in one subsystem where the kink cannot cross through the virtual boundary. Thus we need another method to explain the effect of detachment and attachment to the kink motion.

The Brownian motion of the kink is characterized by two parameters, the drift velocity V_T and the diffusion constant D_T. In the case of TASEP, V_T and D_T are written as [17]

$$V_T = 1 - \lambda_\ell - \lambda_r \quad , \quad D_T = \frac{\lambda_\ell(1 - \lambda_\ell) + \lambda_r(1 - \lambda_r)}{2(\lambda_r - \lambda_\ell)}, \tag{1}$$

where λ_ℓ is the density in the left of the kink and λ_r is the density in the right of the kink which satisfy $\lambda_\ell < \lambda_r$. Thus once λ_ℓ and λ_r are known, the motion of the kink can be determined.

It is known that the Brownian motion in a potential $U(x)$ is written by the Langevin equation

$$\frac{\mathrm{d}x}{\mathrm{d}t} = -\frac{\partial U(x)}{\partial x} + \zeta(t), \tag{2}$$

where $\zeta(t)$ is the random force satisfies

$$\langle \zeta(t) \rangle = 0 \qquad \langle \zeta(t)\zeta(0) \rangle = 2D\delta(t), \tag{3}$$

where $\delta(t)$ is Dirac's delta function. The corresponding Fokker-Plank equation to eq.(2) is

$$\frac{\partial P(x,t)}{\partial t} = \frac{\partial}{\partial x}\left(\frac{\partial U(x)}{\partial x} + D\frac{\partial}{\partial x}\right)P(x,t), \tag{4}$$

where $P(x,t)$ is the probability distribution of the Brownian particle at position x at time t. Equation (4) has the steady solution $P_{st}(x)$

$$P_{st}(x) = C\exp\left[-\frac{U(x)}{D}\right], \tag{5}$$

where C is the normalization constant. We expect that this well-known result can be used to describe the steady distribution of the kink in our model.

For TASEP without detachment and attachment, λ_ℓ and λ_r satisfy

$$\lambda_\ell = \alpha \quad , \quad \lambda_r = 1 - \alpha \tag{6}$$

for $\alpha = \beta < 1/2$. From eq.(1), V_T and D_T are respectively given by

$$V_T = 0 \quad , \quad D_T = \frac{\alpha(1 - \alpha)}{1 - 2\alpha}. \tag{7}$$

If there is a site with detachment and attachment, the phase diagram may be modified from that of the original TASEP. However the difference is expected to be small for small rate of the detachment and attachment ($w_a \sim w_d \ll 1$). Thus the kink picture may be still valid for $\alpha = \beta \ll 1/2$.

Let us consider the kink motion in TASEP with detachment and attachment at one site. If there is no detachment and attachment of particles, λ_ℓ and λ_r are given by
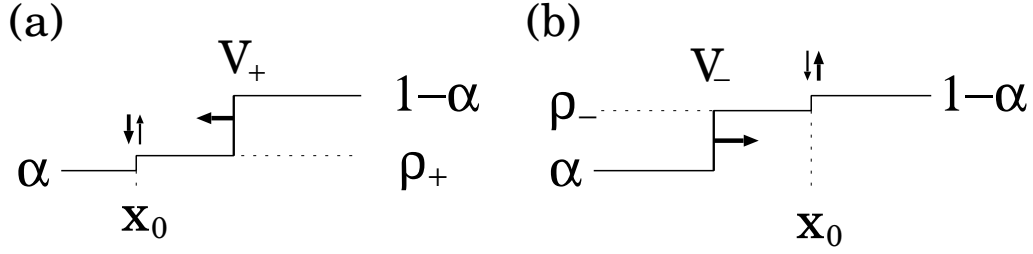
Figure 1. A schematic picture of the kink motion in TASEP with one site of detachment and attachment. The figure (a) shows the case when x_0 is in the low density region of the kink, and the figure (b) shows the case when x_0 is in the high density region of the kink. The line shows the density profile.

eq.(6). However, as a result of detachment and attachment the density is deviated from eq.(6). Let us consider the deviation of the density for two cases :(a) the site of the detachment and attachment is in the low density region of the kink and when (b) the site of detachment and attachment is in the high density region of the kink.

Let us think of the case (a). The density in the left of the kink position x_0 is not affected by detachment and attachment at x_0 but the density in the right of x_0 becomes higher as in the Fig.1(a). This situation takes place because attachment process is likely for low-density region in the one-way motion of the particles. We introduce ρ_+ as the density in the right of x_0 when x_0 is in the low density region of the kink. Thus λ_ℓ should be $\lambda_\ell = \rho_+$ while λ_r is unaffected as $\lambda_r = 1 - \alpha$ when x_0 is in the low density region of the kink.

When x_0 is in the high density region of the kink as in the case (b), the density is affected as in the Fig.1(b). In this case, density in the right of x_0 is not affected by detachment and attachment but the density in the left of x_0 is changed by detachment and attachment. The high density of the particles induce the excess of the detachment current to the attachment current for $w_a \sim w_d$. Thus λ_ℓ and λ_r should be replaced by $\lambda_\ell = \alpha$ and $\lambda_r = \rho_-$ when x_0 is in the high density region of the kink.

Now, let us determine the value of ρ_- and ρ_+. Since the exact solution in the steady state of this model is not known, we adopt the decouple approximation in which the mean currents J_ℓ in the low density region of the kink and J_r in the high density region of the kink are given by $J_\ell = \lambda_\ell(1 - \lambda_\ell)$ and $J_r = \lambda_r(1 - \lambda_r)$ respectively. To estimate ρ_+ and ρ_-, we use the current conservation at the position x_0. For the case when x_0 is in the low density region of the kink, the current from the left of x_0 is $\alpha(1 - \alpha)$ and the current to the right of x_0 is $\rho_+(1 - \rho_+)$. The detach current from x_0 is $w_d\rho_+$ and the attach current at x_0 is $w_a(1 - \rho_+)$. Thus the equation of the current balance at x_0 is given by

$$\alpha(1 - \alpha) + w_a(1 - \rho_+) = w_d\rho_+ + \rho_+(1 - \rho_+). \tag{8}$$

The solution of (8) is simply given by

$$\rho_+ = \frac{1 + w_a + w_d - \sqrt{(1 + w_a + w_d)^2 - 4w_a - 4\alpha(1 - \alpha)}}{2}. \tag{9}$$

Here we use the condition that ρ_+ should be reduced to (6) for $w_a = w_d = 0$. Similarly, the current balance equation of ρ_- is written as

$$\rho_-(1 - \rho_-) + w_a(1 - \rho_-) = w_d\rho_- + \alpha(1 - \alpha), \tag{10}$$

and its solution is given by

$$\rho_- = \frac{1 - w_a - w_d + \sqrt{(1 - w_a - w_d)^2 + 4w_a - 4\alpha(1 - \alpha)}}{2}. \tag{11}$$

From eq.(1) with the consideration around Fig.1, the drift velocities $V_\pm$ are given by,

$$V_+ = \alpha - \rho_+ \quad \text{and} \quad V_- = 1 - \alpha - \rho_-. \tag{12}$$

Similarly the diffusion constants $D_\pm$ are given by

$$D_+ = \frac{\alpha(1 - \alpha) + \rho_+(1 - \rho_+)}{2(1 - \alpha - \rho_+)} \quad \text{and} \quad D_- = \frac{\alpha(1 - \alpha) + \rho_-(1 - \rho_-)}{2(\rho_- - \alpha)}. \tag{13}$$

Here the quantities with the suffix $+/-$ represent those in the right/left of x_0. Using $\lambda_\ell = \alpha, \lambda_r = \rho_-$ for $x < x_0$ and $\lambda_\ell = \rho_+, \lambda_r = 1 - \alpha$ for $x > x_0$, the steady solution of the Fokker-Planck equation can be written as,

$$P(x) = C' \exp\left[\frac{V_-}{D_-}(x - x_0)\theta(x_0 - x) + \frac{V_+}{D_+}(x - x_0)\theta(x - x_0)\right], \tag{14}$$

where C' is a normalization constant, and $\theta(x) = 1$ for $x > 0$ and $\theta(x) = 0$ otherwise.

For $w = w_a = w_d$, the relations

$$\rho_- = 1 - \rho_+ \quad, \quad |V_+| = |V_-| \quad, \quad D_+ = D_- \tag{15}$$

are satisfied. Thus the solution (14) becomes

$$P(x) = C'e^{-\frac{V}{D}|x - x_0|}, \tag{16}$$

where $V = |V_-| = |V_+|$ and $D = D_+ = D_-$. From the comparison of eq.(5) with eq.(16), the potential energy $U(x)$ is given by

$$U(x) = V|x - x_0|. \tag{17}$$

This is one of the main results in this paper. The validity of our theory will be confirmed by Monte-Carlo simulation in section 3.

2.2. Many sites of detachment and attachment

Here we generalize the model in the previous subsection to a model with many sites of detachment and attachment. To ensure the domain wall picture, we assume that $w \doteq w_a = w_d$ are small and the relations eq.(15) are satisfied. Substituting the expansion ρ_+ by w that

$$\rho_+ \simeq \alpha + w + \cdots, \tag{18}$$

we obtain

$$V = w \qquad (19)$$

In this linear regime, we can obtain the probability function of the kink in many sites of detachment and attachment.

Let us consider the system with N sites of detachment and attachment. Thus the system is divided by $N + 1$ segments in which each segment is bounded by the sites of detachment and attachment or the boundaries.

When the kink is located in the jth segment, the number of sites of detachment and attachment in the left of the kink is $j - 1$. For each site of detachment and attachment, the current should be conserved. The density increases by w in the low density region as in the eq.(18) in each segment. Thus the density λ_ℓ in the j-th segment becomes $\lambda_\ell = \alpha + w(j-1)$. On the other hand, the number of sites of detachment and attachment in the right of the kink is $N - j + 1$. Thus the density λ_r in the j-th segment is $\lambda_r = 1 - \alpha - w(N - j + 1)$. Thus, the drift velocity V_j and the diffusion constant D_j in the segment j are respectively given by

$$V_j = w \left\{ N - 2(j - 1) \right\}, \qquad (20)$$

and

$$D_j = \frac{2\alpha(1 - \alpha) + (1 - 2\alpha)wN + w^2((N - j)^2 + j^2)}{2(1 - 2\alpha - wN)}. \qquad (21)$$

Let us omit j-dependence in the eq.(21) by neglecting the term proportional to w^2. Thus the diffusion coefficient is reduced to

$$D = \frac{2\alpha(1 - \alpha) + (1 - 2\alpha)wN}{2(1 - 2\alpha - wN)}, \qquad (22)$$

which is independent of j. From eq.(5), the kink probability distribution $P_j(x)$ in the segment j is given by

$$P_j(x) = C_j \exp \left[-\frac{2w(N - 2(j - 1))(1 - 2\alpha - wN)}{2\alpha(1 - \alpha) + (1 - 2\alpha)wN}(x - x_j) \right], \qquad (23)$$

where C_j is a constant determined from the normalization and the compatibility relation

$$P_j(x_j) = P_{j+1}(x_j). \qquad (24)$$

Thus we obtain the formula applicable to any number of sites of detachment and attachment. It should be noted that the denominator in the exponential function in eq.(23) contain wN. This is because we simply put D in eq.(22) into eq.(5). It may be controversial to contain wN in the denominator as the systematic approximation, but the expression gives us the accurate result as will be shown later.

This method is also applicable to the PFF model[10], where the number of detachment and attachment sites N is $N = L$, the segment length is 1, and the position of the site of detachment and attachment x_j is $x_j = j$. Thus the distribution (23) is

reduced to $P_j(j) = C_j$. We write $P_j = P_j(j)$ for the simplification. The compatibility relation (24) becomes

$$C_j = C_{j-1} \exp\left[\frac{w(L - 2(j-1))}{D}\right], \tag{25}$$

and this recursion relation gives

$$C_j = C_1 \exp\left[\frac{w}{D} \sum_{m=1}^{j-1} (L - 2m)\right]. \tag{26}$$

Thus the distribution is given by

$$P_j = C_1 \exp\left[\frac{w}{D}\left\{-(j - \frac{L+1}{2})^2 + \frac{(L-1)^2}{4}\right\}\right]. \tag{27}$$

This result can be also derived by the superposition of the potential. The harmonic potential is realized by the superposition of the potential (17) as

$$U_{PFF}(j) = \sum_{x_0=1}^{L} w|j - x_0| \simeq w\left(j - \frac{L+1}{2}\right)^2 + \cdots. \tag{28}$$

Thus the distribution of the kink position is given by

$$P_{PFF}(j) = C'' \exp\left[-\frac{w}{D}(j - \frac{L+1}{2})^2\right], \tag{29}$$

where D is given by eq.(22), and the probability distribution function of the kink position (29) is identical to eq.(27).

3. Simulations

Now let us check the quantitative accuracy of our theoretical argument. We compare our analysis with the results of Monte-Carlo simulations. The simulation is carried out by the random update scheme [3, 24], which is realized by choosing the bond between two neighbouring site randomly and move the particle in the chosen sites stochastically.

We use the motion of the second class particle which is a tracer particle of the kink position to detect the kink position [15, 16, 17]. If we write 0 for a hole (empty site), 1 for a particle and 2 for the second class particle, the second class particle moves as $(2,0) \rightarrow (0,2)$ and $(1,2) \rightarrow (2,1)$. The hole is moved to the left of the second class particle, and the particle is moved to the right of the second class particle. Thus the second class particle is positioned between the low density region of particles and the high density region of particles. Thus the second class particle can detect the kink position. We compare the probability function of the kink position obtained by the simulation with the distribution function (14).

As shown in Fig.2, we obtain good agreement between the simulation and the theoretical results in eq.(14). We plot the results of our simulation by $\times$ and the solution of the Fokker-Plank equation by the solid line. The horizontal axis is the kink position and the vertical axis is the probability distribution function of the kink position
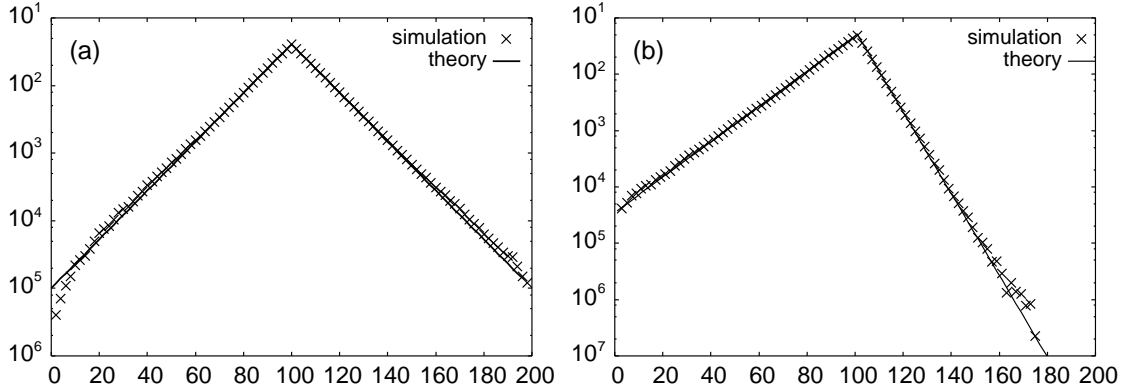
Figure 2. Comparison of the distribution of the kink position between the simulation
($\times$) and the solution of the Fokker-Plank equation (solid line).The horizontal axis is
the kink position and the vertical axis is the distribution function of the kink position
in the steady state plotted in the semi-log scale. The parameters used are $\alpha = \beta = 0.1$
and $w_a = w_d = 0.01$ for (a), and $\alpha = \beta = 0.1, w_a = 0.02$ and $w_d = 0.01$ for (b). We
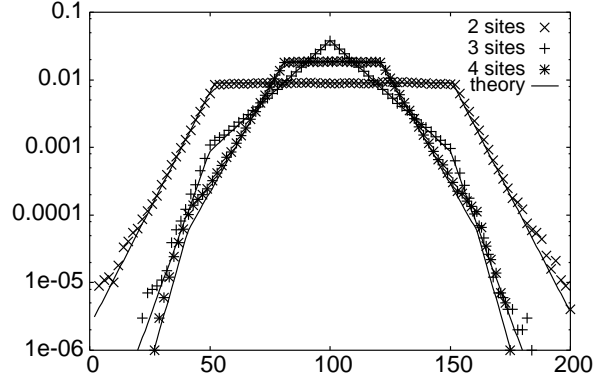set the system length $L = 200$ and the position of detachment and attachment occur
at $x_0 = 100$.

Figure 3. Comparison of the probability distribution of the kink position between
the simulation and the solution of the Fokker-Planck equation (solid lines) in eq.(23)
for the case which has $2(\times)$, $3(+)$ and $4(*)$ sites of detachment and attachment.
The horizontal axis is the kink position and the vertical axis is the probability
function of the kink position in the steady state plotted in the semi-log scale. The
parameters used are $\alpha = \beta = 0.1$ and $w = 0.01$, and the positions of detachment and
attachment are $x_1 = 50, x_2 = 150$ for $N = 2$, $x_i = 50i, (i = 1, 2, 3)$ for $N = 3$ and
$x_i = 40i, (i = 1, 2, 3, 4)$. We set the system length $L = 200$.

in the steady state. In Fig.2(a), the parameter is set to be $w_a = w_d$ and the distribution
function is symmetric around $x = x_0$. In Fig.2(b), the parameter is set to be $w_a \neq w_d$
and the distribution function is asymmetric around $x = x_0$. In both cases, the boundary
parameters are set to be $\alpha = \beta = 0.1$ and the system length L is $L = 200$. In Fig.3, we
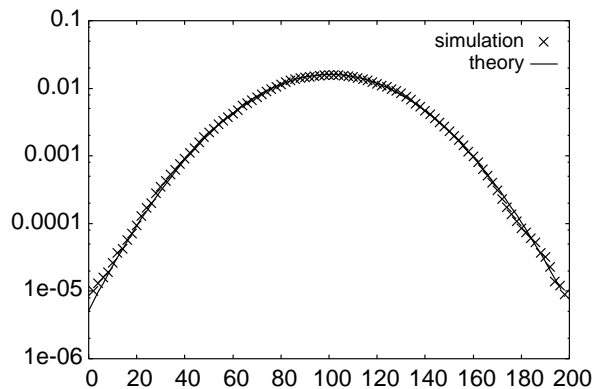compare the theoretical results with the results of our simulation in cases of 2, 3 and 4

Figure 4. Comparison of the probability distribution of the kink position between the simulation ($\times$) and the solution of (eq.(23))the Fokker-Planck equation (solid line) of the PFF model. The horizontal axis is the kink position and the vertical axis is the distribution function of the kink position in the steady state plotted in the semi-log scale. The parameters used are $\alpha = \beta = 0.1, w = 0.0001$ and $L = 200$.

sites of detachment and attachment. The parameters used in this case are $\alpha = \beta = 0.1$ and $w = 0.01$, the position of detachment and attachment are $x_1 = 50, x_2 = 150$ for $N = 2$, $x_i = 50i, (i = 1, 2, 3)$ for $N = 3$ and $x_i = 40i, (i = 1, 2, 3, 4)$. The results of our simulation are plotted by $\times$ for $N = 2$, $+$ for $N = 3$ and $*$ for $N = 4$, and the theoretical results are plotted in the solid lines. In Fig.4, we compare the theoretical results with the simulation results in the PFF model. The parameters at the boundaries are $\alpha = \beta = 0.1$ and $w = 0.0001$. The results of our simulation give quite well agreement of the theoretical prediction in eq.(23) in all cases.

4. Conclusion

We have demonstrated that the kink motion in TASEP with detachment and attachment can be described by the Brownian motion under the influence of the attractive force from detachment and attachment sites. We have obtained the attractive potential to the kink and the diffusion constant of the kink. We demonstrate that the superposition of the potentials of our model gives good results for any number of sites of detachment and attachment when the rates of detachment and attachment are small. We compare our result with the simulation and have confirmed that our theoretical prediction of our theory gives quantitatively correct results. We also explain the reason why the kink in PFF model feels a harmonic potential [19, 20], and succeed the quantitative estimation of the potential.

References

[1] Schütz G M 2001 *Exact Solvable Models for Many-Body Systems Far from Equilibrium, in Phase Transitions and Critical Phenomena* Vol.19 ed Domb C and Lebowitz J L,(Academic,London)

[2] Schmittmann B and Zia R K P 1994 *Statistical Mechanics of Driven Diffusive Systems, in Phase Transitions and Critical Phenomena* Vol.17 ed Domb C and Lebowitz J L,(Academic,London)

[3] Spohn H 1991 *Large Scale Dynamics of Interacting Particles* (Springer-Verlag,New York)

[4] Derrida B,Evans M R,Hakeem V and Pasquier V 1993 *J.Phys.A:Math.Gen* **26** 1493

[5] Schütz G M and Domany E 1993 *J.Stat.Phys* **72** 277

[6] Sasamoto T 1999 *J.Phys.A:Math.Gen* **32** 7109

[7] Uchiyama M, Sasamoto S and Wadati M 2004 *J.Phys.A:Math.Gen* **37** 4958

[8] Helbing D 2001 *Rev.Mod.Phys* **73** 1067

[9] MacDonald C T, Gibbs J H and Pipkin A C 1968 *Biopolimers* **6** 1

[10] Parmeggiani A, Franosch T and Frey E 2003 *Phys.Rev.Lett* **90** 086601

[11] Nishinari K, Okada Y, Schadschneider A and Chowdhury D 2005 *Phys.Rev.Lett* **95** 118101

[12] Kolomeisky A B, Schütz G M, Kolomeisky E B and Straley J P 1998 *J.Phys.A:Math.Gen* **31** 6911

[13] Santen L and Appert C 2002 *J.Stat.Phys* **106** 187

[14] Takesue S, Mitsudo T, and Hayakawa H 2003 *Phys.Rev.*E **68** 015103(R)

[15] Ferrari P A, Kipnis C and Saada E 1991 *Ann.Probab* **19** 226

[16] Ferrari P A 1992 *Prob.Theo.Rel.Fields* **91** 81

[17] Ferrari P A and Fontes L R G 1994 *Prob.Theo.Rel.Fields* **99** 305

[18] Mitsudo T and Hayakawa H 2005 *J.Phys.A:Math.Gen* **38** 3087

[19] Evans M R, Juhász R and Santen L 2004 *Phys.Rev.*E **68** 026117

[20] Juhász R and Santen L 2004 *J.Phys.A:Math.Gen* **37** 3933

[21] Mukherji S and Bhattacharjee S M 2005 *J.Phys.A:Math.Gen* **38** L285

[22] Popkov V, Rákos A, Willmann R D, Kolomeisky A B and Schütz G M 2003 *Phys.Rev.*E **67** 066117

[23] Mirin N and Kolomeisky A B 2003 *J.Stat.Phys* **110** 811 **69** 667

[24] Rajewsky N, Santen L, Schadschneider A and Schreckenberg M 1998 *J.Stat.Phys* **92** 151